*European Journal of Orthodontics* 33 (2011) 113–120
*doi:10.1093/ejo/cjq050*
*Advance Access Publication 13 August 2010*


# Analysis of the performance of different orthodontic devices for mandibular symphyseal distraction osteogenesis

A. Boccaccio*, M. Cozzani** and C. Pappalettere*
*Dipartimento di Ingegneria Meccanica e Gestionale, Politecnico di Bari and **Dipartimento di Ortodonzia, Università degli Studi di Ferrara, Italy

*Correspondence to*: Dr Antonio Boccaccio, Dipartimento di Ingegneria Meccanica e Gestionale, Politecnico di Bari, Viale Japigia 182, 70126 Bari, Italy. E-mail: a.boccaccio@poliba.it

SUMMARY The aim of this study was to investigate the performance of different orthodontic devices for mandibular symphyseal distraction osteogenesis (MSDO). Two performance parameters were analysed, the first of which concerned the stability guaranteed by a distractor in the fracture gap under mastication loads and the second the level of reliability with which a distractor transfers a given expansion to the mandibular bone, inasmuch as the more reliable the device the smaller the difference between the degree of expansion provided to the device and the displacement achieved on the mandibular arch. Hence, a non-linear finite element (FE) model of a human mandible with different devices (tooth-borne, bone-borne, and hybrid) was constructed and then utilized to assess the structural behaviour of the mandibular bone under distraction and mastication loads. An *ad hoc* algorithm was developed to simulate progressive expansion of the devices; a distraction protocol comprising a 10 day latency period and a 6 day distraction period was hypothesized. The first hypothetical expansion given to the device was 2 mm, and the five subsequent expansions were 1 mm.

The results showed that the hybrid device was the most stable appliance under mastication loads, followed by the tooth- and bone-borne devices. However, parasitic rotations of the mandibular arms caused by mastication might counteract the benefits of distraction. The tooth-borne device was found to have the highest reliability in transferring expansion to the mandibular bone. For this device, mandibular expansion was less than the nominal aperture of the distractor by no more than 15 per cent. Lower values of reliability were achieved with the bone-borne device. As the values of the aperture of the appliances increased, the stability guaranteed in the fracture gap increased while the reliability in transferring expansion to the mandibular arch decreased.

## Introduction

Distraction osteogenesis (DO) is a clinical procedure aimed at creating new bone tissue by the gradual separation of two bony segments. Tensile stresses acting on the bone induce and maintain growth and proliferation of the tissue in the direction of the applied forces (Ilizarov, 1989a,b; Costantino *et al.*, 1993). The first report of this technique applied to the craniofacial skeleton was by Snyder *et al.* (1973), who applied DO to a canine mandible. Since the 1990s, DO has become accepted clinical practice for correction of mandibular deficiency and anterior crowding (Guerrero and Contasti, 1992; Guerrero *et al.*, 1997; Weil *et al.*, 1997; Del Santo *et al.*, 2000; Orhan *et al.*, 2003). Histomorphometric analyses has revealed that bone formation in the fracture gap of an osteotomized mandible occurs via intramembranous ossification without substantial intermediate cartilaginous tissue (Loboa *et al.*, 2005). The new bone forms centripetally from the osteotomized bone edges towards the centre of the distraction gap (Loboa *et al.*, 2004).

A number of studies have used the finite element (FE) method to investigate the biomechanics and mechanobiology of mandibular symphyseal (MS) DO. Basciftci *et al.* (2004), using an FE model of a human mandible subjected to midline DO, found that high stress levels were localized in the ramal region. Boccaccio *et al.* (2006) investigated the stress patterns provoked by a tooth-borne device in an osteotomized mandible and observed that the distractor induced stress foci at the fixation points of the device. Nevertheless, the stress peaks were found to be lower than the yield strength of bone. The same authors, using a mechano-regulation algorithm and an FE model of a human mandible, investigated the patterns of tissue differentiation in the fracture gap during both the latency (Boccaccio *et al.*, 2008a) and distraction and post-distraction (Boccaccio *et al.*, 2007) periods. The same model was also utilized to determine how tissue differentiation patterns varied according to age (Boccaccio *et al.*, 2008b). Loboa *et al.* (2004, 2005) carried out a study on the mechanobiology of DO using a rat model submitted to hemimandibular osteotomy. They compared the histological findings with the strain and pressure fields predicted by an FE model of an osteotomized mandible and observed that tensile strains of up to 13 per cent corresponded to regions of new bone.

A variety of MS DO appliances are currently available. However, these can be reduced to three principal types: tooth borne, bone borne, and hybrid (Conley and Legan, 2003). The principal difference between these appliances is the location of the insertion points into the mandibular arch (Conley and Legan, 2003). The tooth-borne device is attached to the teeth, the bone-borne device to the basal bone, and the hybrid device to both the basal bone and teeth. Among the performance parameters that an orthodontic device should exhibit, two have crucial relevance. The first of these is the stability that a distractor should guarantee in the fracture gap. If rigidity is not ensured, micro-fractures may occur within the regenerate bone, and this may result in focal haemorrhaging and cartilage interposition (Imola, 2004). Furthermore, inadequate stabilization leads to poor vascularization of the callus and subsequently to a slower healing process (Lienau *et al.*, 2005). However, excessive stabilization is undesirable. The flexibility of the distractor arms allows micro-movements to occur within the fracture gap, thus stimulating osteogenetic activity and bone regrowth (Bell *et al.*, 1999). The second performance parameter is the reliability with which the appliance transfers expansion to the mandibular bone. The fact that a given aperture is applied to the distractor does not necessarily imply that the same displacement is transferred to the mandible. Ideally, points localized in the osteotomized region would displace to the same (or, at least, as similar as possible) degree as the nominal expansion applied to the device. The first of the above performance parameters will hereinafter be referred to as 'stability' and the second as 'displacement reliability'.

In a previous study (Boccaccio *et al.*, 2008c), a FE model was used to predict the structural response of an osteotomized mandible fitted with a tooth-borne, bone-borne, or hybrid device under functional loads. The model provided quantitative information concerning the stability and displacement reliability of the investigated devices. In the present research, the model was further developed in order to determine the change in stability and displacement reliability with different device apertures at different time points subsequent to day 0 when the osteotomy was performed. A 10 day latency period followed by a 6 day distraction period with a frequency of one distraction per day was hypothesized. An *ad hoc* algorithm was generated to simulate the changes in mandibular geometry induced by progressive distraction and the consequent alteration in the load transfer pattern in the osteotomized region.

## Materials and methods

### *FE models*

Computer tomographic scan data (slice thickness 1 mm, pixel size 0.42 mm) were used in the creation of the FE model of a human mandible. Data processing was performed using Mimics® software, version 7.2 (Materialise Inc., Leuven, Belgium). Non-uniform rational B-spline surfaces delimiting the shape of the virtual model were generated by the MedCAD® module provided with Mimics®. Mandibular geometry was discretized into FEs (i.e. divided into volumetric sub-domains) by means of FEMAP® software (Siemens PLM Software Inc., Munich, Germany). Three-dimensional models of the three distractors were constructed using the Pro/Engineer Wildfire™ CAD environment, version 2.0 (Parametric Technology Corporation, Needham, Massachusetts, USA). The mandible and distractors were assembled in Abaqus® (Hibbit, Karlsson and Sorensen, Providence, Rhode Island, USA), where FE analyses were performed (Figure 1). More than 100 000 four-node tetrahedral elements were employed to mesh the complex geometry of the mandibular arch and orthodontic appliances. A 2 mm-thick callus (Meyer *et al.*, 2004) was introduced between the two mandibular rami of the model (Figure 2). Further details of the FE discretization and the simplifications adopted have been reported (Boccaccio *et al.*, 2008c).

### *Boundary conditions*

Four different boundary conditions were simulated.

Boundary condition (i) mimicked the presence of the temporomandibular joint (TMJ; Figure 3a). Two reference points representing the condyles were placed at the location

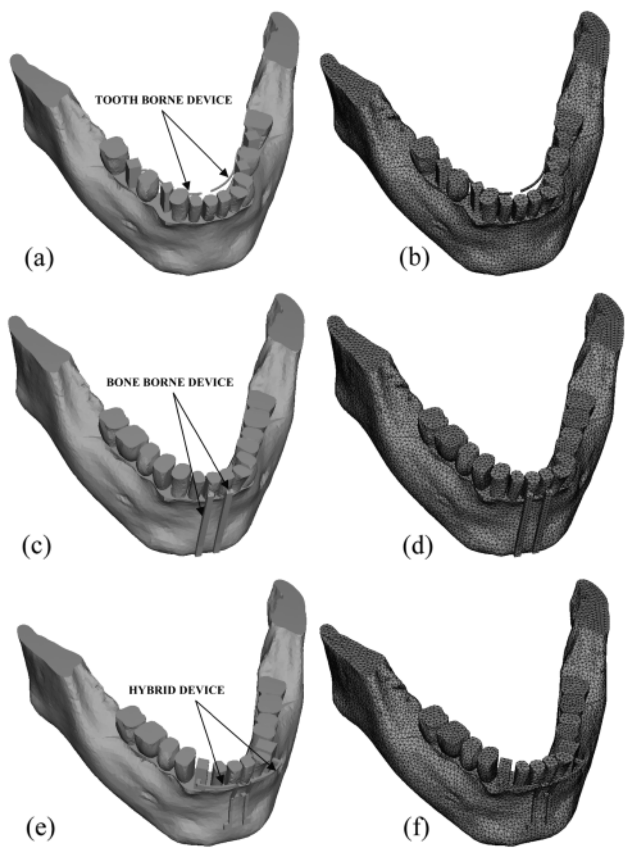


**Figure 1** Three-dimensional computer-aided design model (left) and finite element mesh (right) of the mandible fitted with the tooth-borne (a, b), the bone-borne (c, d), and the hybrid (e, f) devices.

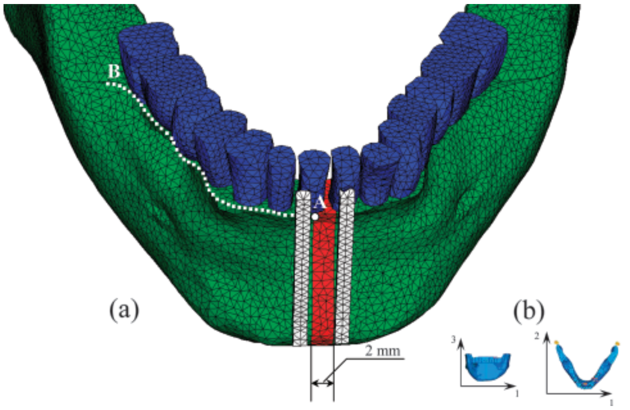


**Figure 2** (a) The osteotomized region: the bone-borne device is highlighted in white, the bone callus in red, the teeth in blue, and the cortical bone in green; the hatched white line indicates the control path AB along which the displacement values were plotted; (b) reference system used in the finite element analyses.

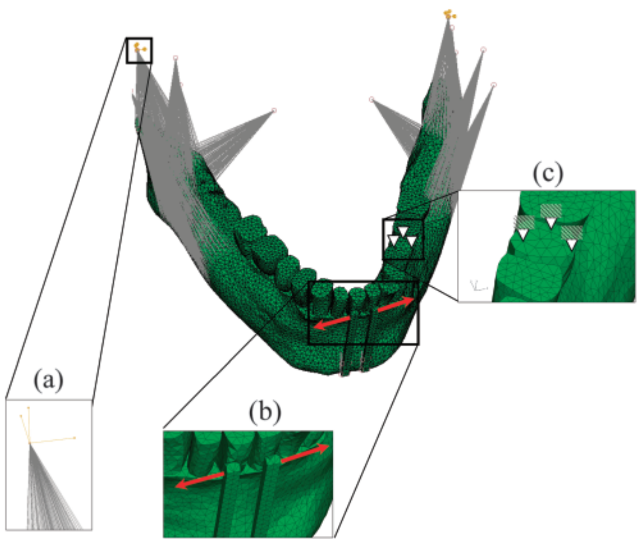


**Figure 3** Boundary and loading conditions utilized in the finite element analyses: (a) the coupling constraint used to model the temporomandibular joint; (b) the displacement field to which the device was subjected; (c) the constraints utilized to simulate unilateral occlusion.

of the articulation. Mandibular arms were connected to the reference points by means of coupling constraints. The behaviour of the TMJ disc was modelled by constraining these reference points to three fixed points by means of spring elements aligned to the coordinate system. Thus, the mandibular arms were able to rotate about the line limited by the reference points and translate along coordinate directions. Boundary condition (ii) modelled the mastication phase. The actions of the most important muscles involved in the mastication process, masseter, temporalis, and pterygoid were included (Figure 3). The loads were applied at the points of insertion of the muscles into the mandibular bone. Force amplitude and direction were taken from Faulkner *et al.* (1987). Boundary condition (iii) simulated unilateral occlusion on the second premolar on the left mandibular arm (Figure 3c). The action of chewing was modelled on the mandibular arch by constraining the second premolar with simple supports preventing $u_3$ displacement (i.e. the component of the displacement vector $\vec{u}$ in direction 3; Figure 2b). Finally, boundary condition (iv) reproduced the aperture process of the distractor (Figure 3b).

### *Material properties*

Five different regions were distinguished within the model: (1) cancellous bone, (2) cortical bone, (3) teeth, (4) distractor, and (5) bone callus. All materials were modelled as homogeneous, isotropic, and linear elastic. Table 1 lists the values of the mechanical properties used in the FE analysis of cancellous bone, cortical bone, distractor, and teeth. Computation of Young's modulus of the bone callus on the first day of distraction was based on the results reported by Mora and Forriol (2000), who measured the equivalent stiffness $K$ (Newton per millimetre) of the bone callus formed in osteotomized sheep bone in which the fractured parts had been re-joined by means of external fixators.

Following the hypothesis that the first distraction given to the device occurs 10 days after the osteotomy, i.e. a protocol with a 10 day latency period was adopted, a Young's modulus $E$ of 0.385 MPa can be computed. Calculation of Young's modulus of the bone callus in the following 5 days of hypothetical distraction was based on the trend derived from a mechano-regulation model developed in a previous study (Boccaccio *et al.*, 2007), which describes the change in $E$ over time. This model predicts the patterns of tissue differentiation in the fracture gap during the distraction period based on the value of the biophysical stimulus acting on the mesenchymal tissue. It also predicts how the mechanical properties change over time and, moreover, provides information about the equivalent Young's modulus exhibited by the entire fracture gap, day by day, during the distraction period. These values were utilized in the present study and implemented in the algorithm described below.

### *Algorithm*

An *ad hoc* algorithm, of which a graphical summary is depicted in Figure 4, was generated in FORTRAN environment in order to simulate the process of expansion during the distraction period. The algorithm included six iterations, each of which

**Table 1** Material properties utilized in the finite element analyses

| Material | Young's modulus (GPa) | Poisson's ratio |
|---|---|---|
| Cancellous bone* | 1.37 | 0.3 |
| Cortical bone* | 13.7 | 0.3 |
| Teeth* | 18.6 | 0.31 |
| Distraction appliances | 210 | 0.3 |

*Pegoretti *et al.* (2002).

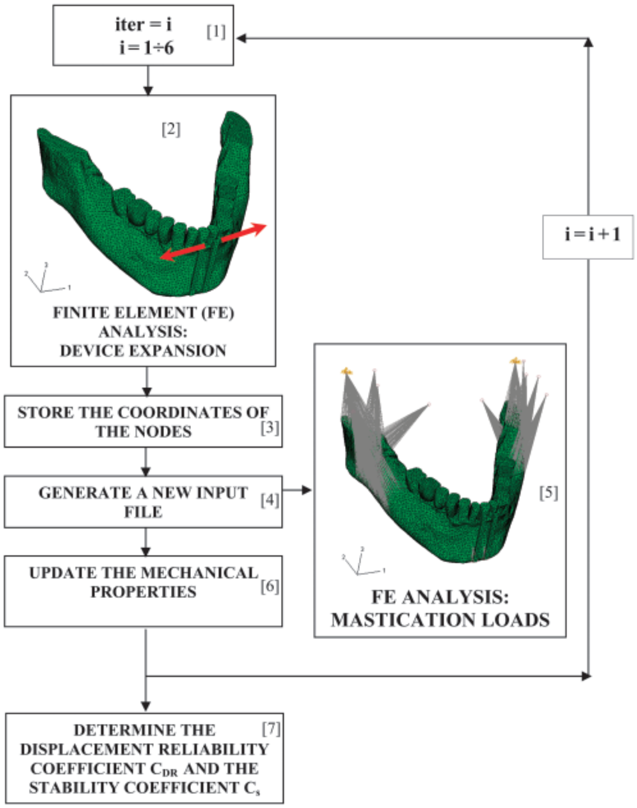


**Figure 4** Schematic of the implemented algorithm

corresponded to a single hypothetical distraction of the device. When the first iteration was initiated [Block (1)], a non-linear FE analysis was performed [Block (2)] in which only boundary conditions (i) and (iv) were activated. The expansion of the orthodontic device was simulated, with a nominal aperture given to the appliance in this first iteration of 2 mm. All nodes of the mandible model were displaced and their spatial coordinates ($x$,$y$,$z$) changed. These new coordinates were then stored [Block (3)] and used to create a second model $M_{\text{distracted}}$ [coded in an input file; Block (4)]. Subsequently, a second, non-linear FE analysis was performed [Block (5)] on $M_{\text{distracted}}$, this time including activation of boundary conditions (i), (ii), and (iii), so as to investigate changes in the expansion of the mandibular arch when subjected to mastication loads (in addition to constraints simulating unilateral occlusion). At this point, the Young's modulus of the fracture gap was updated for $M_{\text{distracted}}$ [Block (6)], according to the rules described previously, and a new iteration initiated. The nominal expansion given to the device in iterations 2–6 was 1 mm. When all the iterations had been completed, the algorithm calculated two different coefficients, which served to quantify the performance of the distractor in terms of stability and displacement reliability.

If $u^{\text{A}}_{1,\text{mastication\_iter}=i}$ is the displacement along direction 1 (Figure 2b) at point A (located on the right edge of the osteotomy) in the $i$th iteration in the presence of mastication and $u^{\text{A}}_{1,\text{no\_mastication\_iter}=i}$ is the same quantity in the absence of mastication, the stability coefficient $C_{\text{S}}$ is expressed as follows:

$$C_{\text{s}} = \frac{u^{\text{A}}_{1,\text{mastication\_iter}=i}}{u^{\text{A}}_{1,\text{no\_mastication\_iter}=i}} \times 100. \qquad (1)$$

Thus, if $C_{\text{S}}$ is equal to 100 per cent, no difference exists between the presence and absence of mastication loads. This is equivalent to saying that the displacement measured at point A is insensitive to mastication or that no displacement occurs within the regenerate tissue when mastication loads are applied. In such a case, it is possible to define the distractor as 'stable'. The stability exhibited by the device decreases as smaller values of $C_{\text{S}}$ are predicted.

If $\delta_{\text{device\_iter}=i}$ is the nominal aperture given to the device at the $i$th iteration (with $i$ in the interval 1–6), the displacement reliability coefficient $C_{\text{DR}}$ is defined as follows:

$$C_{\text{DR}} = \frac{u^{\text{A}}_{1,\text{no\_mastication\_iter}=i}}{\delta_{\text{device\_iter}=i}} \times 100. \qquad (2)$$

If $C_{\text{DR}}$ = 100 per cent, no difference therefore exists between the expansion given to the device at the $i$th iteration and the displacement transferred to the mandible during the same iteration. The greater this difference is with respect to zero the smaller the values of $C_{\text{DR}}$ are computed.

The algorithm shown in Figure 4 was implemented for all three orthodontic devices investigated.

## Results

The trend of $u_1$ displacement (i.e. the component of the displacement vector $\vec{u}$ along direction 1; Figure 2b) was determined along the indicated control path AB (Figure 5). The control path AB was considered to lie along the buccal bony marginal ridge (BBMR; Figure 2a), as DO creates additional space in the vicinity of this region into which the teeth, initially (before DO) in intimate contact, can be repositioned.

For each aperture given to the device, two curves were plotted: the first was obtained in the presence and the second in the absence of mastication. Interestingly, in the vicinity of point A, the displacement values predicted in the presence of mastication were always smaller than those predicted in its absence.

Maps of the $u_1$ displacement field were visualized (in the absence of mastication) for the different apertures given to each distractor (Figure 6).

Finally, the trends of the above-mentioned coefficients, $C_{\text{DR}}$ and $C_{\text{S}}$, were traced for each different aperture of the distractors (Figure 7). A quadratic regression curve, with the corresponding regression coefficient $R^2$, was added to each diagram. It appears that as expansion increased, decreasing values of $C_{\text{DR}}$ and increasing values of $C_{\text{S}}$ were predicted.

## Discussion

In this study, analysis of the performance of different distraction devices was carried out. The FE model of an

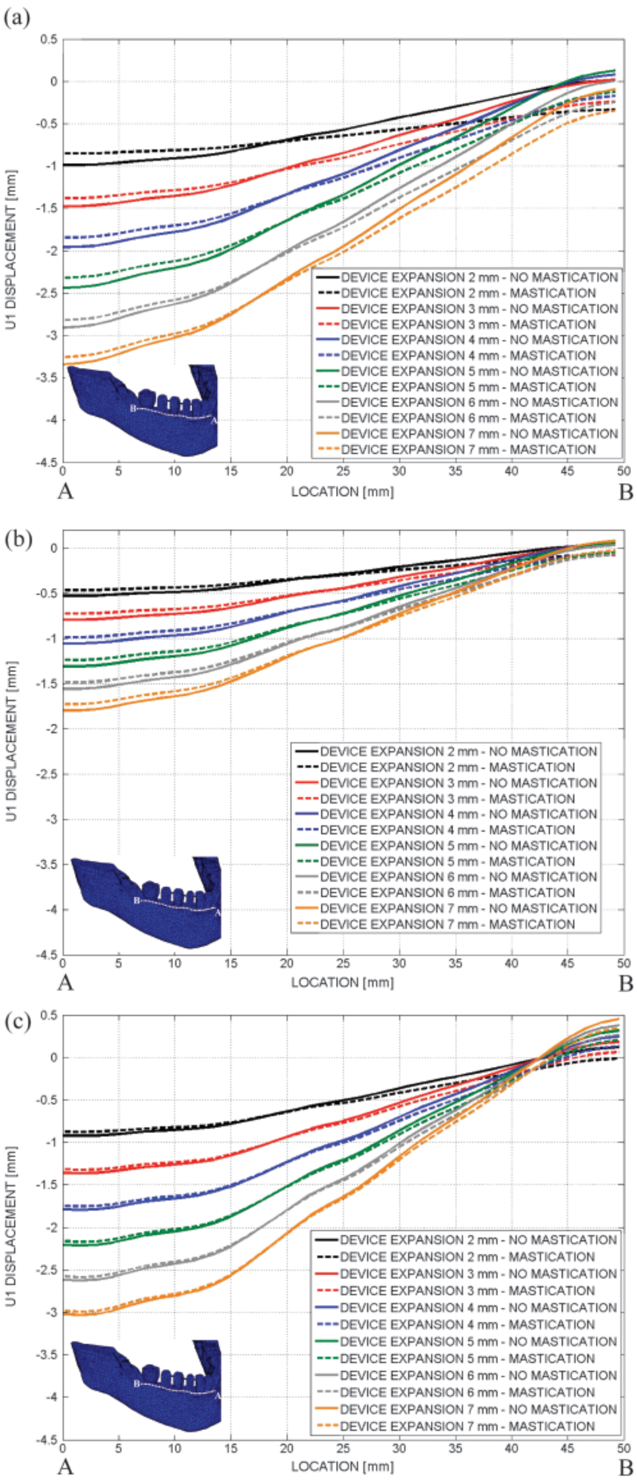


**Figure 5** Trend of the $u_1$ displacement along the control path AB for the tooth-borne (a), the bone-borne (b), and the hybrid (c) devices.

osteotomized human mandible with different devices was used to predict the structural behaviour of the mandibular bone under distraction and mastication loads. Two coefficients were defined to quantitatively express the performance exhibited by each appliance.

The present model had some limitations. First, a simplified model of the TMJ was utilized, and the coupling constraints and spring elements used to simulate this articulation do not accurately portray the actual behaviour of such a complex joint (Beek *et al.*, 2000). Furthermore, a simplified approach was adopted to compute the change over time of the mechanical properties of the bone callus. However, despite these limitations, the values of the displacement reliability coefficient $C_{DR}$ appear to be in good agreement with those found *in vivo* by Loboa *et al.* (2004), who distracted rat mandibles at a frequency of 0.5 mm/day over an 8 day period. Upon completion of treatment, an average aperture of 3.36 mm, against the 4 mm of nominal aperture given to the device, was measured for the bone callus, thereby yielding a $C_{DR}$ coefficient of 84 per cent. Moreover, as demonstrated by Boccaccio *et al.* (2006), the FE model of the osteotomized mandible utilized in this study predicted displacements, at given control points, consistent with those measured *in vivo* by Weil *et al.* (1997) and Del Santo *et al.* (2000). Indeed, percentage variation of the interdental distance (at the canines, first premolars, second premolars, first molars, and second molars) predicted by the FE model consistently fell within the standard deviations exhibited by the experimental data reported in the literature. Moreover, the trend lines of *in vivo* measurements (Weil *et al.*, 1997; Del Santo *et al.*, 2000) generally appear to agree with the numerical predictions. In addition, the model predicted a slight decrease in bigonial width following distraction. This result is consistent with the clinical data reported by Malkoç *et al.* (2006), who evaluated the effects of MSDO on dental and mandibular skeletal structures with tooth- and bone-borne devices. They found that a small decrease in bigonial width occurs approximately 11 days after surgery. Furthermore, the present model predicted a significant increase in distance between the left and right mandibular central and lateral incisors, in agreement with the *in vivo* measurements of Malkoç *et al.* (2006). Second, the materials incorporated were considered as homogeneous and isotropic, whereas the mandibular bone is generally inhomogeneous and anisotropic. However, according to Marinescu *et al.* (2005), such a simplification does not significantly affect the accuracy of the predicted results. Finally, the model predicted the displacement field experienced by the mandibular bone and calculated the performance of the orthodontic appliances in the days following surgery. An evaluation of the long-term effects of DO on mandibular structures (Işeri and Malkoç, 2005) would be a worthwhile addition to future models.

The values of $u_1$ displacement along path AB were plotted for each of the investigated appliances (Figure 5). It appears that the displacement predicted near point A (located on the edge of the osteotomy) was smaller in the presence of mastication than that predicted without mastication. This can be explained by parasitic rotations produced by the masticatory muscles, in opposition to those produced by the distractors, affecting the mandibular arch (Figure 8). The values of displacement predicted by

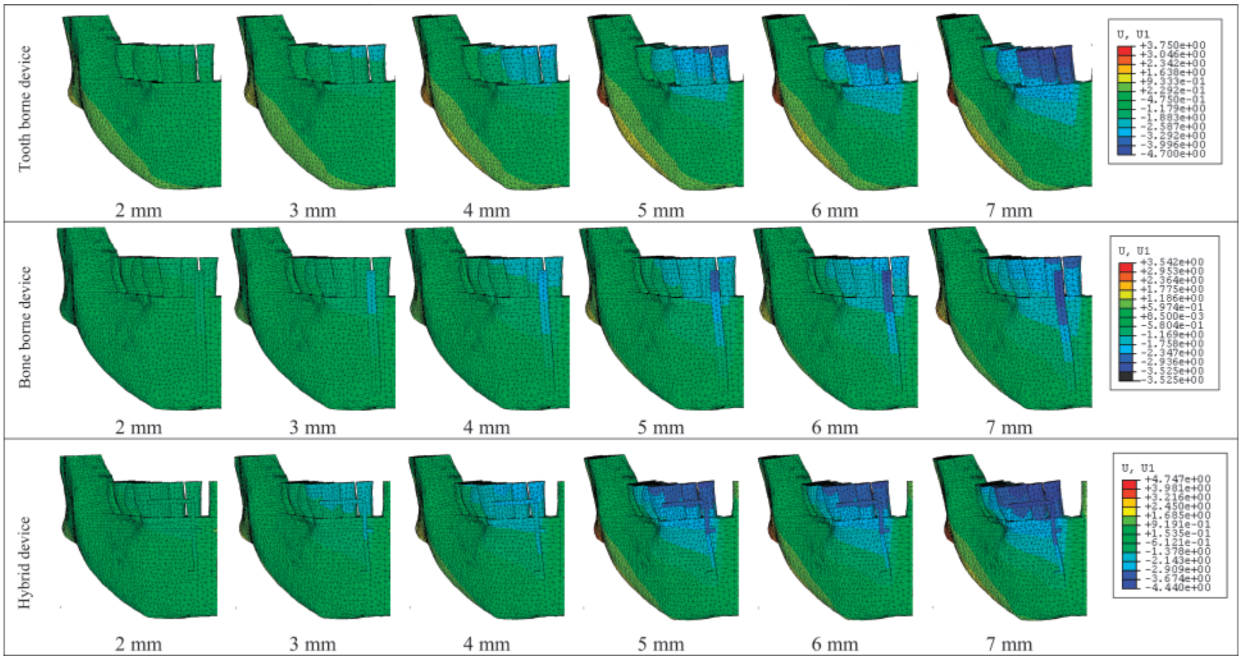


**Figure 6** $u_1$ displacement maps for the different distraction devices and for different apertures.

the FE model decreased from the anterior towards the posterior side. This behaviour is consistent with the findings of Basciftci *et al.* (2004), who observed that the greatest widening is achieved at the symphyseal region and that the widening effect gradually diminishes from the anterior to the posterior. Furthermore, the displacements predicted for the bone-borne device were generally smaller than those predicted for the other two appliances, presumably because with the bone-borne device, the displacement is transferred (from the device to the mandibular arch) through fixation points located on the basal bone. In contrast, for the tooth-borne and hybrid devices, at least one fixation point (for each mandibular ramus) is attached to the teeth, and therefore, a greater amount of dental/dentoalveolar expansion can occur. In other words, for these devices, a greater amount of expansion occurs in the vicinity of the BBMR, where the control path AB lies. Further evidence of this can be gleaned from Figure 6, which illustrates maps of the $u_1$ displacement field. The expansion recorded on the dental arch for the tooth-borne and hybrid devices appears to be more significant (highlighted with different shades of blue) than that predicted for the bone-borne device.

The highest values of the displacement reliability coefficient $C_{DR}$ were predicted for the tooth-borne device (Figure 7a–c). This is due to both fixation points (on each mandibular ramus) of this appliance being located close to the BBMR. However, the difference between the $C_{DR}$ exhibited by the tooth-borne device and that exhibited by the hybrid device never exceeded 11 per cent. Values of $C_{DR}$ significantly lower than those predicted for the tooth-borne and the hybrid devices were found for the bone-borne appliance.

Interestingly, for all the three device concepts investigated, as the expansion of the appliance increased, decreasing values of the displacement reliability coefficient $C_{DR}$ were predicted. This is because, as distraction proceeds, the stiffness of the mandibular arches counteracts expansion of the device, and thus, the displacement at point A becomes smaller than the aperture of the device.

The most stable appliance appears to be the hybrid device (Figure 7d–f), presumably due to the fact that, for this device, the fixation points are located both on the basal bone and on the teeth. Indeed, the points located on the teeth allow controlled displacement of mandibular points on the arch (i.e. where control point A is situated); the fixation points located on the basal bone permit reduction in the parasitic rotations produced by the masticatory muscles. Nevertheless, a high degree of stability was also computed for the tooth- and bone-borne devices. In fact, the difference between the values of $C_S$ predicted for the hybrid device and those predicted for the other two appliances never exceeded 10 per cent.

Increasing values of the stability coefficient $C_S$ were predicted for increasing apertures of the devices. This occurred because, as distraction proceeds, the lever arm of the resultant mastication force is lowered, resulting in smaller values of the bending moment acting on the fracture gap. Figure 9 shows a schematic representation of the mandibular bone viewed from above (continuous line). The action of all the muscles involved in mastication can be reduced to a resultant force $F$. The component $F_v$ of $F$, perpendicular to the transverse plane (i.e. the plane upon which the representation was drawn), generates a bending moment at point Q, where the bone callus is located, given

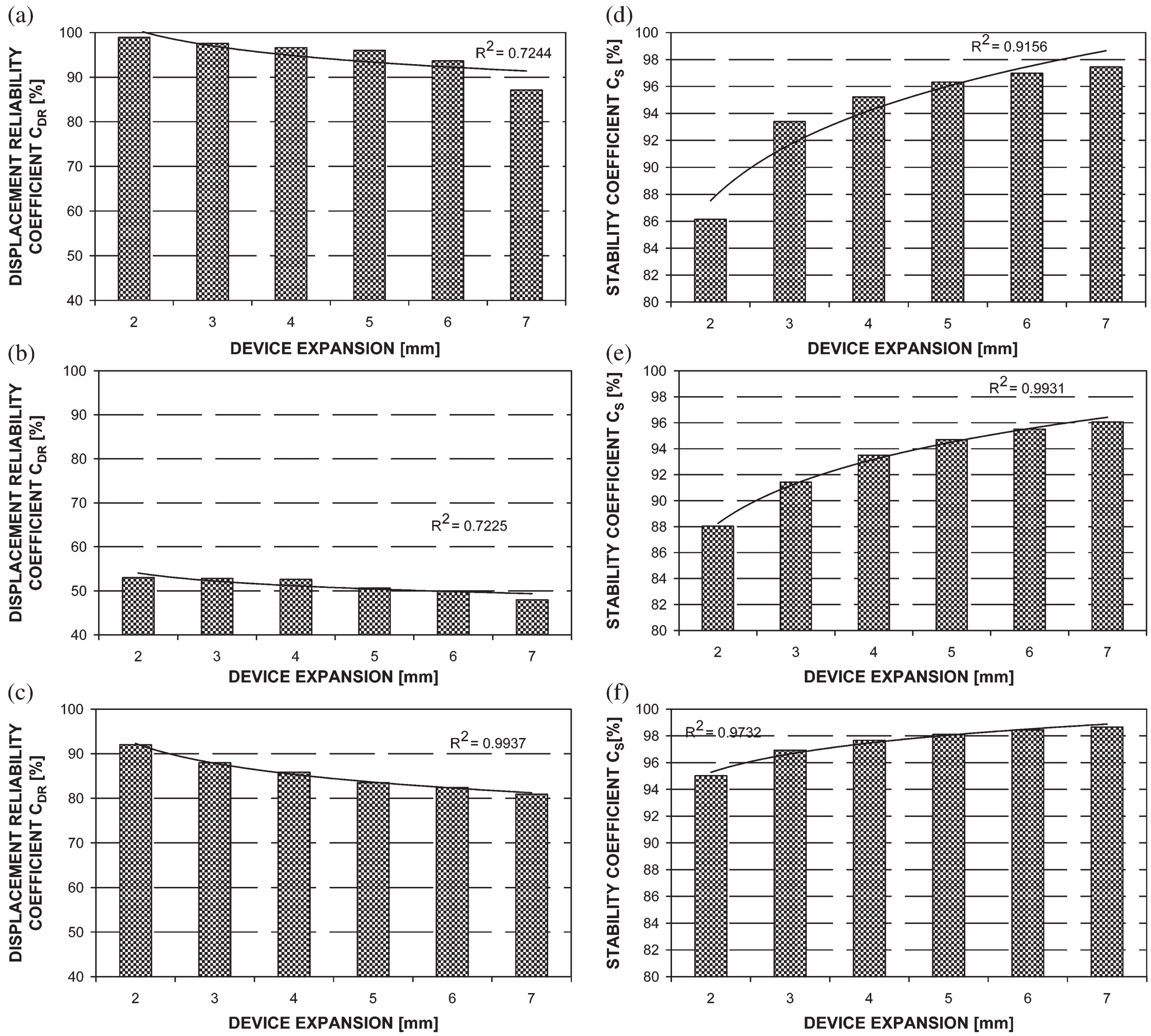


**Figure 7** Displacement reliability coefficient $C_{DR}$ for the tooth-borne (a), the bone-borne (b), and the hybrid (c) devices. The displacement reliability coefficient $C_{DR}$ is defined as the ratio between the displacement along direction 1 at point A in the absence of mastication and the nominal aperture of the device. Stability coefficient $C_S$ for the tooth-borne (d), the bone-borne (e), and the hybrid (f) devices. The stability coefficient $C_S$ is defined as the ratio between the displacement along direction 1 at point A in the presence of mastication and the same in the absence of mastication.

by $M = F_V b$. After distraction (dashed line), the lever arm $b$ becomes $b'$, and the bending moment $M'$ assumes the form $M' = F_V b'$, with $M' < M$. In other words, as distraction proceeds, the effect of the parasitic rotations generated by the muscular forces become less significant, and thus, greater stability can be achieved under mastication loads.

The quadratic curve utilized to interpolate the values of $C_S$ and $C_{DR}$ for all the appliances investigated seems to be well suited to describing the change in these coefficients for different apertures of the device.

## Conclusions

In this study, a comparison of the performance of different orthodontic devices was carried out. Specifically, the stability in the fracture gap guaranteed by the appliances and the reliability with which the appliance transfers expansion to the mandibular bone were investigated. Two different coefficients were defined to quantitatively express these performance parameters. An *ad hoc* algorithm was generated to simulate progressive distraction of the devices; a distraction protocol with a 10 day latency period and a 6 day distraction period was hypothesized. The results show that the stability in the fracture gap increases while the displacement reliability decreases as the distraction proceeds. Under these conditions, the hybrid device appeared to be the most stable. However, the tooth-borne device, although less stable under mastication loads, resulted in similar displacement to that of the distractor alone.

**Figure 8** The parasitic rotation (continuous line) produced on the mandible by the mastication muscles is opposite to that (dashed line) produced by the distractor.

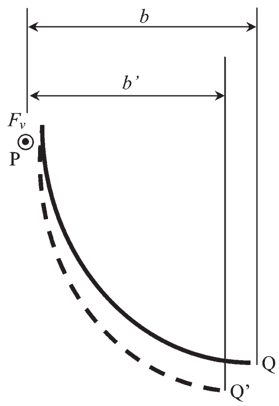


**Figure 9** Schematic of the mandibular bone (continuous line) viewed from above. The muscular action can be reduced to a concentrated force *F* applied at a point P close to the mandibular condyle. The vertical component $F_V$ (perpendicular to the transverse plane) generates a moment with respect to point Q (close to the osteotomized region) given by $M = F_V b$, where *b* is the lever arm. As the distraction occurs (dashed line), the lever arm decreases (*b* becomes *b*′) and then the moment decreases consequently.

## References

Basciftci F A, Korkmaz H H, Işeri H, Malkoç S 2004 Biomechanical evaluation of mandibular midline distraction osteogenesis by using finite element method. American Journal of Orthodontics and Dentofacial Orthopedics 125: 706–715

Beek M, Koolstra J H, Van Ruijven L J, Van Eijden T M G J 2000 Three-dimensional finite element analysis of the human temporomandibular joint disc. Journal of Biomechanics 33: 307–316

Bell W H, Gonzalez M, Samchukov M L, Guerrero C A 1999 Intraoral widening and lengthening of the mandible in baboons by distraction osteogenesis. Journal of Oral Maxillofacial Surgery 57: 548–562

Boccaccio A, Lamberti L, Pappalettere C, Carano A, Cozzani M 2006 Mechanical behaviour of an osteotomized mandible with distraction orthodontic devices. Journal of Biomechanics 39: 2907–2918

Boccaccio A, Pappalettere C, Kelly D J 2007 The influence of expansion rates on mandibular distraction osteogenesis: a computational analysis. Annals of Biomedical Engineering 35: 1940–1960

Boccaccio A, Prendergast P J, Pappalettere C, Kelly D J 2008a Tissue differentiation and bone regeneration in an osteotomized mandible: a computational analysis of the latency period. Medical and Biological Engineering & Computing 46: 283–298

Boccaccio A, Lamberti L, Pappalettere C 2008b Effects of ageing on the latency period in mandibular distraction osteogenesis: a computational mechano-biological analysis. Journal of Mechanics in Medicine and Biology 8: 203–225

Boccaccio A, Lamberti L, Pappalettere C, Cozzani M, Siciliani G 2008c Comparison of different distraction orthodontic devices: a finite element study. American Journal of Orthodontics and Dentofacial Orthopedics 134: 260–269

Conley R, Legan H 2003 Mandibular symphyseal distraction osteogenesis: diagnosis and treatment planning considerations. Angle Orthodontist 73: 3–11

Costantino P D, Friedman C D, Shindo M L, Houston C G, Sisson G A 1993 Experimental mandibular regrowth by distraction osteogenesis. Long term results. Archives of Otolaryngology-Head & Neck Surgery 119: 511–516

Del Santo M, Guerrero C A, Buschang P H, English J, Samchukov L, Bell W 2000 Long-term skeletal and dental effects of mandibular symphyseal distraction osteogenesis. American Journal of Orthodontics and Dentofacial Orthopedics 118: 485–493

Faulkner M G, Hatcher D C, Hay A 1987 A three-dimensional investigation of temporomandibular joint loading. Journal of Biomechanics 20: 997–1002

Guerrero C A, Contasti G I 1992 Transverse (horizontal) mandibular deficiency. In: Bell W H (ed). Modern practice in orthognathic and reconstructive surgery Saunders, Philadelphia, pp. 2383–2397.

Guerrero C A, Bell W H, Contasti G I, Rodriguez A M 1997 Mandibular widening by intraoral distraction osteogenesis. British Journal of Oral and Maxillofacial Surgery 35: 383–392

Ilizarov G A 1989a The tension stress effect on the genesis and growth of tissues: part I, the influence of stability of fixation and soft tissue preservation. Clinical Orthopaedics 238: 249–261

Ilizarov G A 1989b The tension stress effect on the genesis and growth of tissues: part II, the influence of the rate and frequency of distraction. Clinical Orthopaedics 238: 263–285

Imola J M 2004 Craniofacial distraction osteogenesis. (http://www.emedicine.com/ent/topic702.htm) (25 May 2010, date last accessed)

Işeri H, Malkoç S 2005 Long-term skeletal effects of mandibular symphyseal distraction osteogenesis. An implant study. European Journal of Orthodontics 27: 512–517

Lienau J, Schell H, Duda G N, Seebeck P, Muchow S, Bail H 2005 Initial vascularization and tissue differentiation are influenced by fixation stability. Journal of Orthopaedic Research 23: 639–645

Loboa E G *et al.* 2004 Mechanobiology of mandibular distraction osteogenesis: experimental analyses with a rat model. Bone 34: 336–343

Loboa E G *et al.* 2005 Mechanobiology of mandibular distraction osteogenesis: finite element analyses with a rat model. Journal of Orthopaedic Research 23: 663–670

Malkoç S, Işeri H, Karaman A I, Mutlu N, Küçükkolbaşi H 2006 Effects of the mandibular symphyseal distraction osteogenesis on mandibular structures. American Journal of Orthodontics and Dentofacial Orthopedics 130: 603–611

Marinescu R, Dealing D J, Rapoff A J 2005 Finite element modeling of the anthropoid mandible: the effect of altered boundary conditions. The Anatomical Record Part A 283: 300–309

Meyer U, Kleinheinz J, Joos U 2004 Biomechanical and clinical implications of distraction osteogenesis in craniofacial surgery. Journal of Cranio-Maxillofacial Surgery 32: 140–149

Mora G, Forriol F 2000 Mechanical analysis of the healing of different osteotomies fixed externally. International Orthopaedics 24: 295–298

Orhan M, Malkoç S, Usumez S, Uckan S 2003 Mandibular symphyseal distraction and its geometrical evaluation: report of a case. Angle Orthodontist 73: 194–200

Pegoretti A, Fambri L, Zappini G, Bianchetti M 2002 Finite element analysis of a glass fibre reinforced composite endodontic post. Biomaterials 23: 2667–2682

Snyder C C, Levine G A, Swasson H M, Browne E Z 1973 Mandibular lengthening by gradual distraction: preliminary report. Plastic and Reconstructive Surgery 51: 506–508

Weil T S, Van Sickles J, Payne J 1997 Distraction osteogenesis for correction of transverse mandibular deficiency: a preliminary report. Journal of Oral and Maxillofacial Surgery 55: 953–960